

---

# Wind tunnel measurements of the aerodynamic forces on Renson louvre blades

Tim De Troyer (FLOW/VUB, Pleinlaan 2, 1050 Brussel)

December 30, 2018

---

## Contents

1	Introduction	3
2	Experimental setup	3
2.1	The VUB low-speed wind tunnel . . . . .	5
2.2	The aerodynamic balance . . . . .	6
2.3	The device under test . . . . .	6
3	Results and discussion	7
3.1	Measurement procedure . . . . .	7
3.2	Data processing . . . . .	7
4	Conclusions	9
5	Appendix	10
6	Louvre blade: L03301	11
7	Louvre blade: L03301	12
8	Louvre blade: L03301	14
9	Louvre blade: L03301	15
10	Louvre blade: L03301	16
11	Louvre blade: L03301	17
12	Louvre blade: L03301	18

13 Louvre blade: L033CL	19
14 Louvre blade: L033CL	20
15 Louvre blade: L033IM1	22
16 Louvre blade: L033IM1	23
17 Louvre blade: L033HF	25
18 Louvre blade: L033HF	26
19 Louvre blade: L05000	28
20 Louvre blade: L05000	29
21 Louvre blade: L050CL	31
22 Louvre blade: L050CL	32
23 Louvre blade: L050IM1	34
24 Louvre blade: L050IM1	35
25 Louvre blade: L050W	37
26 Louvre blade: L050W	38
27 Louvre blade: L050WS	40
28 Louvre blade: L050WS	41
29 Louvre blade: L060AC	43
30 Louvre blade: L060AC	44
31 Louvre blade: L060HF	46
32 Louvre blade: L060HF	47
33 Louvre blade: L060HF	49
34 Louvre blade: L060HF	50
35 Louvre blade: L060HF	51
36 Louvre blade: L06606	52

37 Louvre blade: L06606	53
38 Louvre blade: L066CL	55
39 Louvre blade: L066CL	56
40 Louvre blade: L066IM1	58
41 Louvre blade: L066IM1	59
42 Louvre blade: L066V	61
43 Louvre blade: L066V	62
44 Louvre blade: L075W	64
45 Louvre blade: L075W	65
46 Louvre blade: L12001	67
47 Louvre blade: L12001	68
48 Louvre blade: ICR06601	70
49 Louvre blade: ICR06601	71
50 Louvre blade: ICP03301	73
51 Louvre blade: ICP03301	74
52 Summary of all results	76

## 1 Introduction

The Vrije Universiteit Brussel (VUB) was asked by Renson to perform experimental measurements of the lift and drag coefficients of a set of louvre blades (hereafter referred to as *blades*) in its wind tunnel. This report summarises the results of this measurement campaign, executed in August and September 2017.

The tested scale model blades are listed in Table 1. All measurements are performed twice, once of only the blade, and once with the blade in between an array of the same blades (to replicate real-life conditions). The array assures that the wind flow around the blade, and thus the angle of attack, is similar to that of a set of blades mounted on the wall of a building.

## 2 Experimental setup

**Table 1:** The list of blades that have been tested during the measurement campaign, together with the reference length (which is the projected height of the blade) used for the calculation of the lift and drag coefficients.

Name	$c$ (mm)
L.033.01	37.5
L.033CL	37.5
L.033IM1	37.5
L.033HF	37.5
L.050.00	56
L.050CL	60
L.050IM1	60
L.050W	89.6
L.050WS	50.5
L.060AC	69
L.060HF	60
L.066.06	73
L.066CL	76.5
L.066IM1	76.5
L.066V	74
L.075W	101
L.120.01	120
ICR.066.01	76.5
ICP.033.01	37.5

## 2.1 The VUB low-speed wind tunnel

The low-speed wind tunnel of the Vrije Universiteit Brussel is an open-circuit blow-down wind tunnel originally developed for environmental testing. A centrifugal fan is driven by a 50 kW frequency-controlled motor. The air is settled through two screens and a honeycomb at the entrance of the settling chamber.

The test section is 2 m wide, around 1 m high (the height increases along the test section, to compensate for a growing boundary layer), and 9 m long. The maximum speed in the test section is 20 m/s. The turbulence intensity is about 0.5 % at 10 m/s. The test section is followed by a small diffuser and an exhaust that deflects the flow upwards. A general overview of the wind tunnel is given in Figure 1.



**Figure 1:** General overview of the wind tunnel. Clockwise from top left: the settling chamber, the centrifugal blower, the test section, and the diffuser with exhaust.

The wind speed is measured with BnC-Lambrecht 630a pitot tubes. The pitot tubes are connected to a SETRA Model 239 differential pressure sensor, which measures the dynamic pressure. Pressure, temperature, and relative humidity are measured as well to calculate the air density. All sensors are connected to a National Instruments PCI-6221 board and registered using LabVIEW. All sensors are recalibrated annually.

## 2.2 The aerodynamic balance

The wind tunnel is equipped with a 6-axis force-torque sensor from ME Meßsysteme, Type K6D154 100N/10Nm, hereafter referred to as the aerodynamic balance. This balance has been recalibrated in June 2017, specifically for this measurement campaign. The readings of the balance are synchronously measured with the aerodynamic parameters using LabVIEW.

## 2.3 The device under test

The set-up of the blades and arrays have been built by Renson according to specifications given by VUB. The aerodynamic balance is installed on top of the floor of the test section. The blade is mounted on top of the aerodynamic balance, such that the blade is entirely outside the wind tunnel boundary layer. A floating floor is mounted around the blade to avoid any interference effect of the balance on the blade. (The boundary layer height on this floor is very small, under 5 mm, and its effect can be neglected.)

The array, if present, is mounted on top of the floating floor, around the blade. Care is taken to assure that the blade and the array do not touch, so that only the forces on the blade are measured by the aerodynamic balance. On top of the array, a small plate is foreseen to avoid tip effects.

For two specific cases, L.033.01 and L.060.HF, a back plate was installed at distances of 20 mm, 46 mm, and 100 mm, to simulate the effect of a wall. Figure 2 shows an example of the most complete setup (with array and back plate), while Figure 3 shows a different setup (without back plate), which was the most commonly tested configuration.

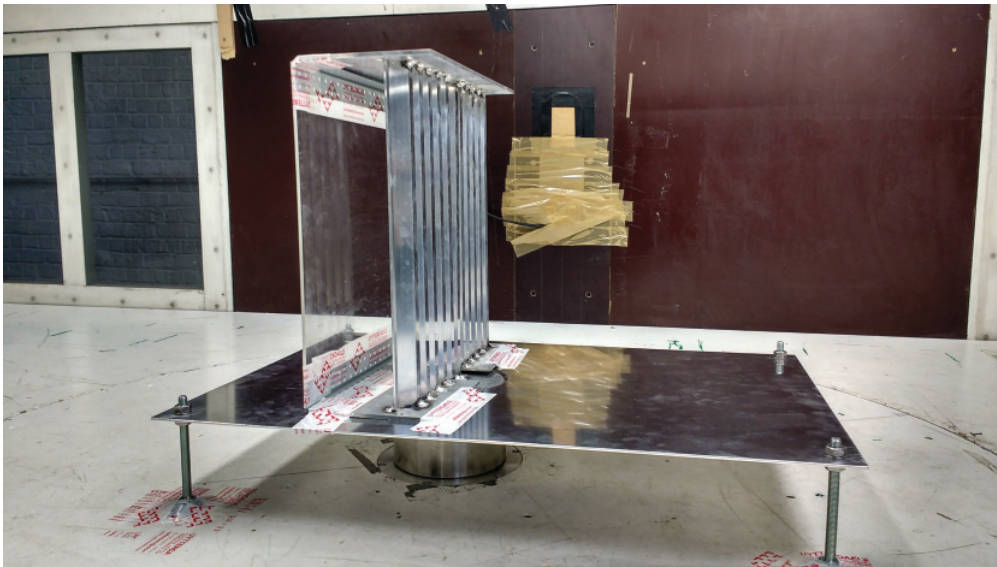


**Figure 2:** Example of the most complete set-up, including the blade mounted on top the aerodynamic balance (the metal cylinder below the floating floor), the array mounted on top of the floating floor, and the back plate here at 100 mm.

---

All blades were manufactured with the same *span* (or length) of 390 mm.

For blade type L.033.01, three different orientations with respect to the incoming wind were





**Figure 3:** Example of the most set-up with array but without end plate, which was the most commonly tested configuration. The photograph is taken looking downstream towards the exit louvres.

tested:  $0^\circ$ ,  $45^\circ$  and  $90^\circ$ . (Here,  $0^\circ$  means that the set-up is perpendicular to the wind, as shown in Figure 2.) As the highest forces were measured for  $0^\circ$ , this orientation was assumed to be the worst-case scenario; therefore, all subsequent tests have been done with this orientation.

### 3 Results and discussion

#### 3.1 Measurement procedure

Measurements were typically performed at two wind speeds, 10 m/s and 16 m/s. The force coefficients, as they are normalised by the square of the wind speed, should be identical (within the error margin) for the different wind speeds. This was almost always so. For these cases, only the values at 16 m/s were put in the summarising table, as these have the lowest error bars.

For a limited number of cases (often of the CL or IM type), the force coefficients differed more than the error margin. This was invariably caused by the deformation of the array under the wind load (resulting in physical contact between the array and the test blade), and consequently erroneous readings by the aerodynamic balance. In these cases, the measurements were repeated at different wind speeds, and typically a clear change in the trend of the coefficients (as a function of wind speed) could be found (see e.g. Figure 4). We then selected the highest wind speed before the trend change as the value to be included in the summarising table.

#### 3.2 Data processing

The aerodynamic balance was programmed to measure forces and moments about the centre of the blade under test. The lift and drag forces were then obtained by a simple rotation from the axis of the balance to the axis of the wind tunnel. The drag force,  $F_x$ , is defined as positive

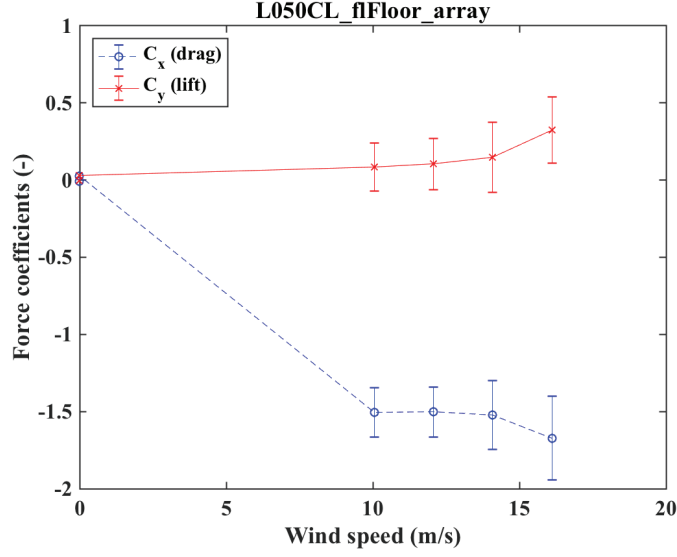


**Figure 4:** Example of a case (the L.050.CL with array) where the deformation of the array caused erroneous measurements beyond 12 m/s.

upstream. (Therefore, all drag values are expected to have a negative sign.) The lift force,  $F_y$  is defined as positive to the left (looking upstream). A schematic top view is provided in Figure 5.

Given that the blades are measured at a  $90^\circ$  angle, a positive lift force corresponds to a downwards force for real-life, horizontally-installed blades.

The lift and drag coefficients are obtained by normalising the forces with the dynamic pressure, the blade span,  $b$ , and a reference length,  $c$ :

$$C_x = \frac{F_x}{\frac{1}{2}\rho V^2 bc} \quad (1)$$

$$C_y = \frac{F_y}{\frac{1}{2}\rho V^2 bc} \quad (2)$$

where  $\rho$  is the air density and  $V$  the wind tunnel speed.

For all cases, the reference length  $c$  was the projected height of the blade, as specified by Renson (and reprinted in Table 1 for completeness).

Confidence bounds on the measured lift and drag coefficients were calculated through linear error propagation of the measurement uncertainty on the forces, wind speed, density, length, and angle measurements. The dominant source of uncertainty is the measurement precision of the aerodynamic balance ( $\pm 0.2$  N in  $x$  and  $\pm 0.3$  N in  $y$ , both with probability 95 %), which is relatively high for the low forces on the blades (which are in the order of a few newton). Therefore, the highest wind speeds have been used (with the highest forces) where possible, as these result in the lowest uncertainty. The confidence bounds have then been calculated for a confidence level of 95 % by assuming a Gaussian distribution. They are denoted by  $\epsilon$  in the table.

Every stored force measurement is an average over 5000 samples, which corresponds to a



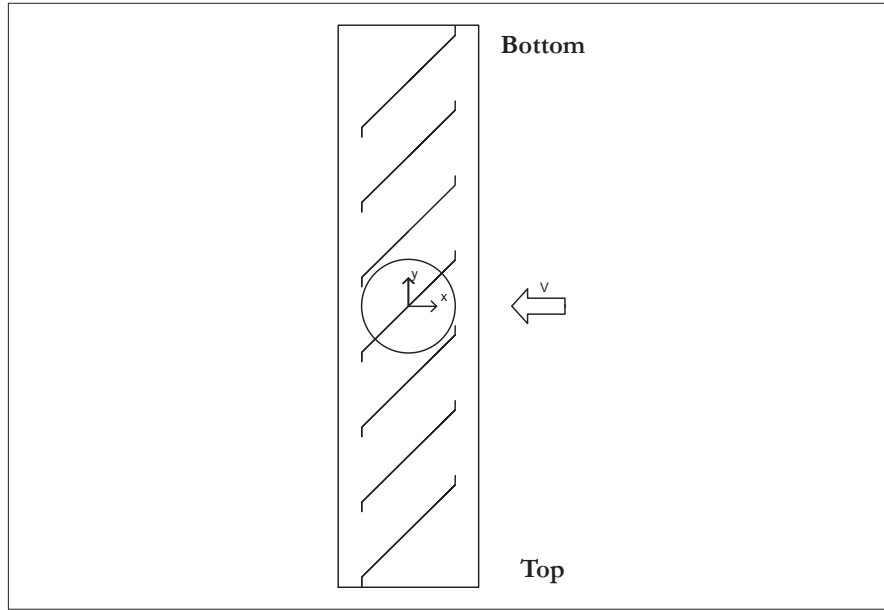


**Figure 5:** Schematic top view of the setup for a fictive blade, indicating the direction of the wind speed and the definition of the  $x$  and  $y$  axes.

measurement time of about 1 minute per wind speed. For some blades, however, the forces varied heavily in the course of this 1 minute (see e.g. L.050W), and thus some instantaneous forces were considerably higher than the mean value. To quantify this variation, the summarising table also lists the standard deviation normalised by the mean value of the force (in the  $x$  and  $y$  directions respectively), the so-called coefficient of variation (CV, in the table expressed as a percentage). This value can be used to predict the instantaneous peak forces that can be expected, which can be useful for prudent calculations.

## 4 Conclusions

Lift and drag coefficients have been derived from experimental force measurements in the wind tunnel. These data have been presented, together with confidence intervals and the coefficient of variation.

## 5 Appendix

The appendix shows the measurement information in tabular and graphical format.

The measurement ID provides information about the context of the measurement:

- *fFloor* implies that a vertical bottom plate has been used (this is the case for all measurements included,
- *array* implies that the blade was measured in between an array of blades (while, if *array* is not added, the blade was measured in isolation),
- *bWall\_Xmm* implies that a solid back wall was mounted behind the blades, at a distance of X mm,
- *angleXX* indicates that the setup was rotated clockwise over XX degrees.

The table displays the force coefficients  $C_x$  and  $C_y$ , the wind speed  $V$  (m/s), the reference length  $c$  (mm), the 95 % confidence bounds on the force coefficients ( $\epsilon_x$  and  $\epsilon_y$ , respectively), and the coefficient of variation ( $CV_x$  and  $CV_y$ , respectively, in %). The  $x$  direction is positive upstream; a negative value of  $C_x$  corresponds thus to a positive drag coefficient. The  $y$  direction is positive to the left (when looking upstream); a positive value of  $C_y$  corresponds to a downwards lift force for horizontally-mounted louvre blades. A CAD drawing is included for every tested configuration, indicating the direction of the wind and the orientation of  $x$  and  $y$ .

### 13 Louvre blade: L033CL

Measurement ID: L033CL<sub>flFloor</sub>

$C_x$	$C_y$	$V$ (m/s)	$c$ (mm)	$\epsilon_x$	$\epsilon_y$	$CV_x$ (%)	$CV_y$ (%)
-1.47	0.79	10.12	37.50	0.20	0.18	16.37	5.00
-1.48	0.77	16.20	37.50	0.20	0.21	6.29	2.02

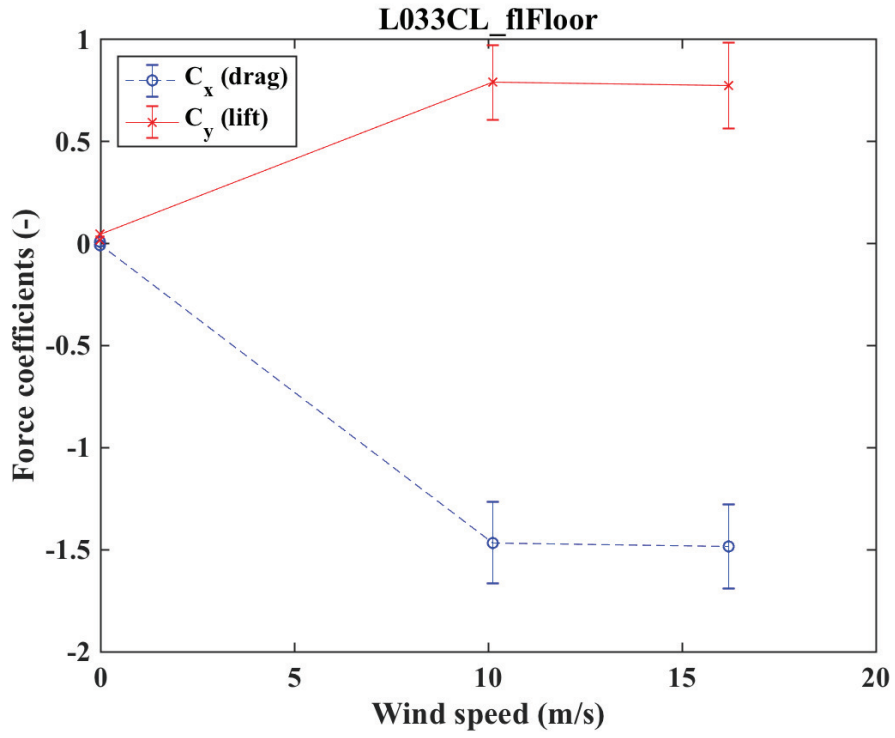


Figure 13: L033CL<sub>flFloor</sub>

## 14 Louvre blade: L033CL

Measurement ID: L033CL<sub>flFloorarray</sub>

$C_x$	$C_y$	$V$ (m/s)	$c$ (mm)	$\epsilon_x$	$\epsilon_y$	$CV_x$ (%)	$CV_y$ (%)
-1.67	0.12	10.05	37.50	0.22	0.19	15.76	16.61
-2.61	0.18	16.11	37.50	0.37	0.29	3.93	4.14
-1.72	0.19	6.01	37.50	0.46	0.36	41.56	41.06
-1.69	0.16	8.03	37.50	0.28	0.23	23.95	24.30
-2.15	0.12	12.07	37.50	0.36	0.28	8.64	9.30
-2.41	0.13	14.07	37.50	0.43	0.32	5.67	6.11

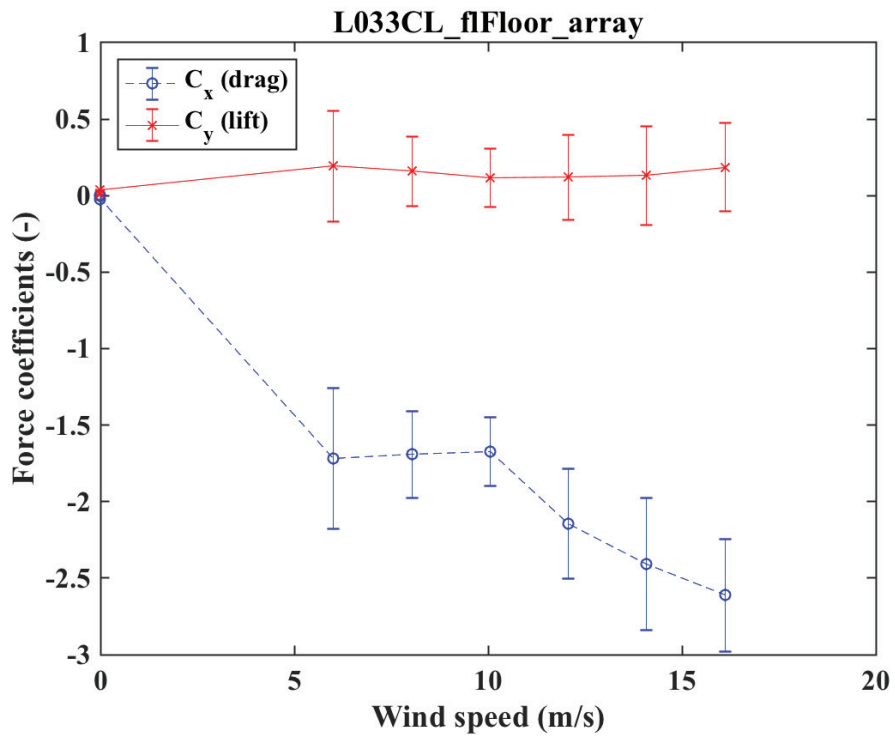
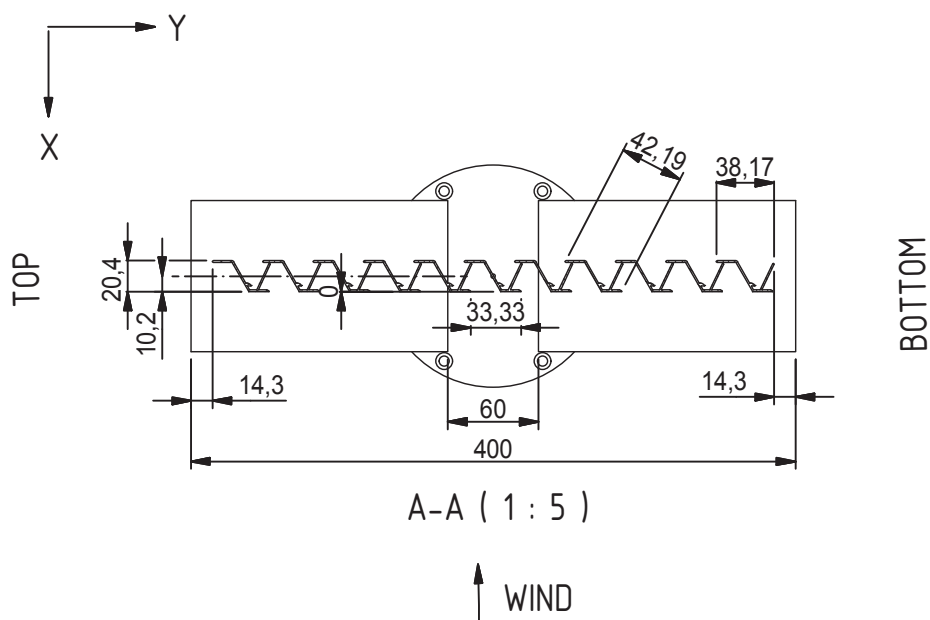
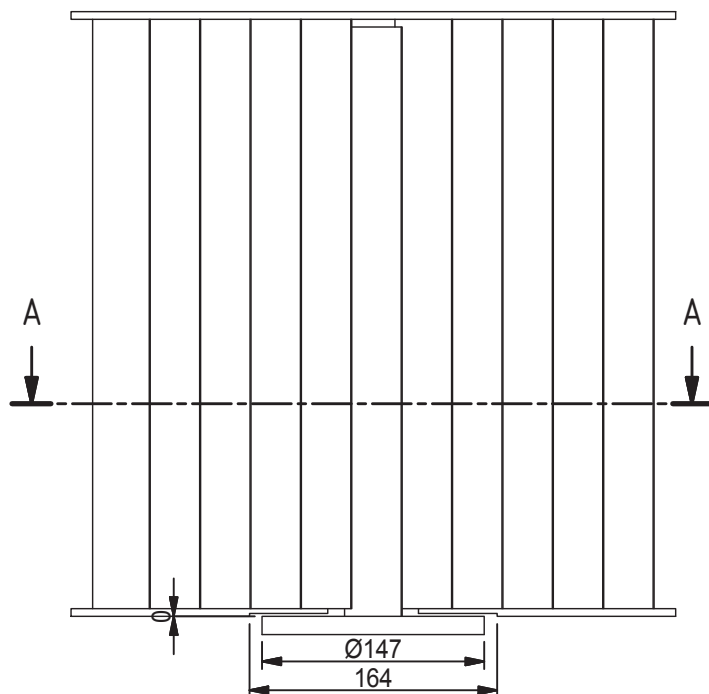



Figure 14: L033CL<sub>flFloorarray</sub>



OPGELET : DEZE TEKENING GELDT VOOR ZOWEL LAMEL L.030CL EN L.030IM1

Mat. :		Finish :		Weight : <i>N/A</i>		Area :		Volume : <b>883,416 cm³</b>		Base part :		Tol. : <b>DIN 2768mk</b>									
 <a href="http://www.renson.eu">www.renson.eu</a> - 8790 Waregem (Belgium)  This drawing is owned by RENSON and may not be copied or shown to third parties without written permission.				Description :								Sheet : <b>1 / 1</b>									
				L.033CL en L.033IM1 testopst. gecombin.								Scale : <b>1 : 5</b>									
												Drawn : <b>Bconi</b>									
				Use. :								Part. nr. :		Revision :		State : <b>Released</b>		Creation date : <b>7/07/2017</b>		Size : <b>A4</b>	
								r0075723								-		Doc. nr.: <b>r0075723</b>		units in mm	

www.renson.eu - 8790 Waregem (Belgium)

This drawing is owned by RENSON and may not be copied or shown to third parties without written permission.